Supplementary Information for

Including fluorescent nanoparticle probes within injectable gels for remote strain measurements and discrimination between compression and tension

Hannah R. Shanks, Shanglin Wu, Nam T. Nguyen, Dongdong Lu and Brian R. Saunders*

School of Materials, University of Manchester, MSS Tower, Manchester, M13 9PL, U.K.

Movie S1.

Kneading of the PEI-MG gel

The method for mechanical kneading of the PEI-MG is shown in this video. Note that the PL probe particles were not added during the preparation of the gel shown in this movie. The process followed when the probe particles are added is the same as shown in this video, with the exception that the probe dispersions are added sequentially after the PEI solution and before mixing begins as described in the Experimental section.

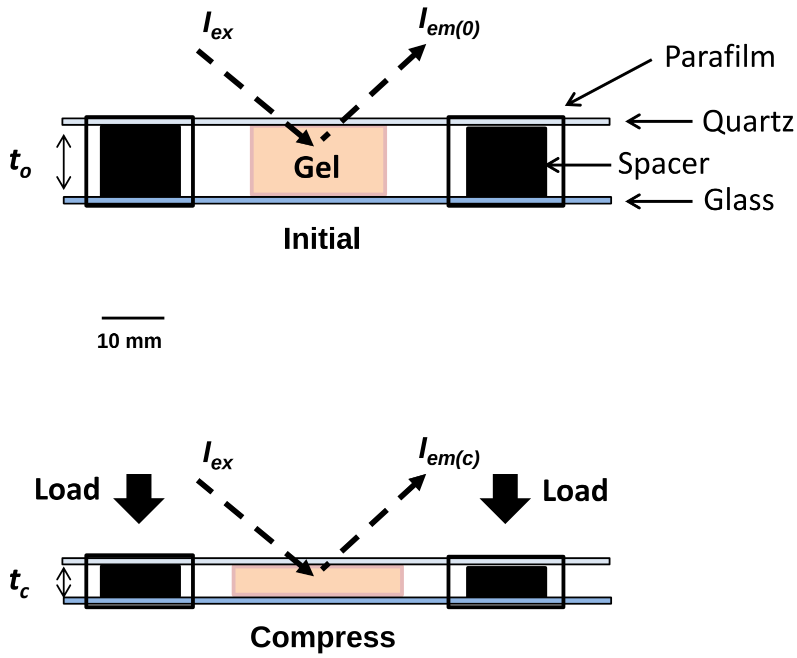

Figure S1. Schematic diagram showing how the gels were compressed whilst measuring the PL emission spectra. I_{ex} and I_{em} are the intensities of the excitation and emission beams.

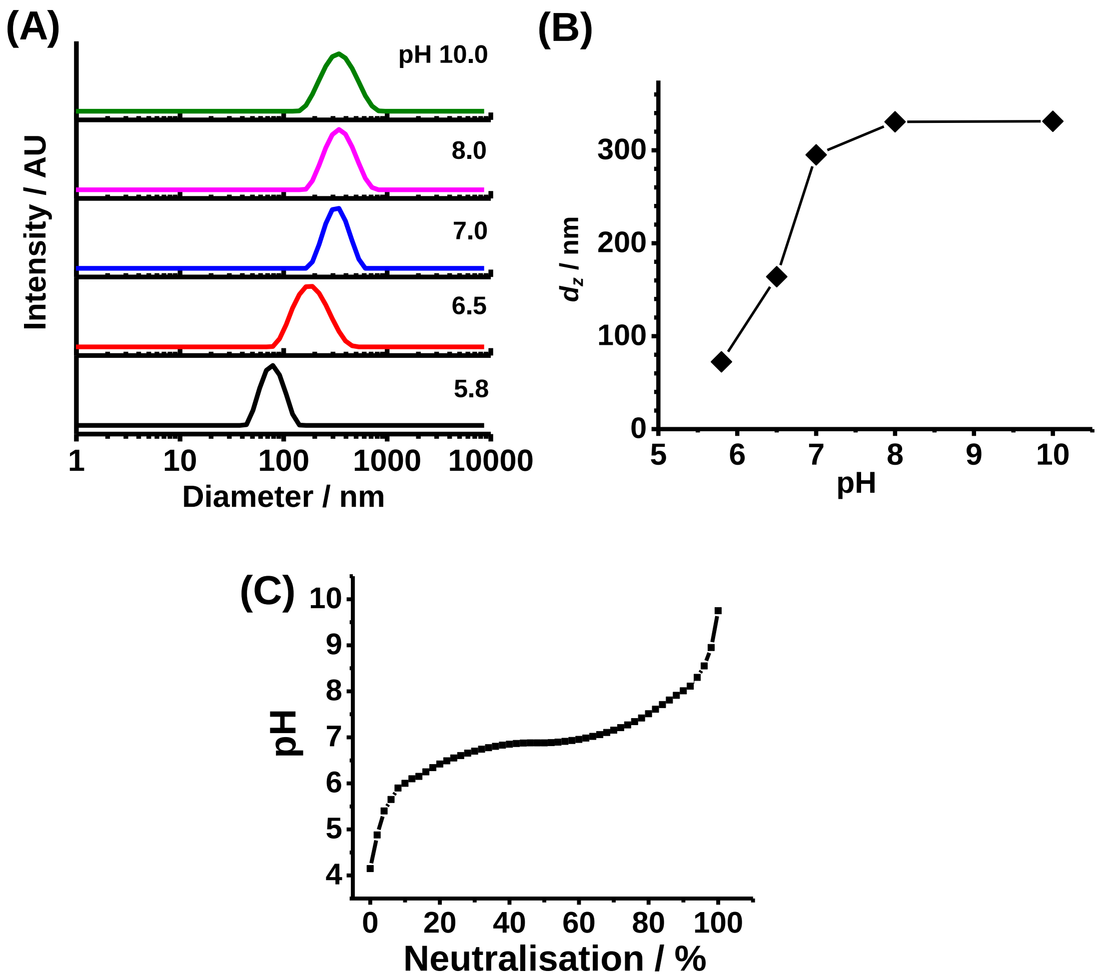

Figure S2 DLS size distributions (**A**) and z-average diameter as a function of pH (**B**) for the CF particles. (**C**) Titration data for the CF dispersion.

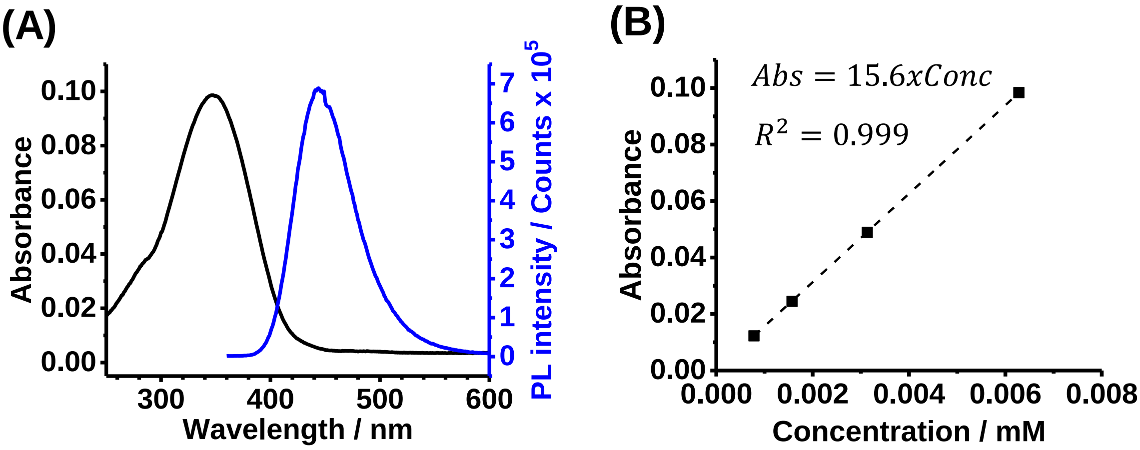

Figure S3 **(A)** UV-visible and PL spectra for CF350. **(B)** Concentration dependence of the absorbance measured at the absorption maximum in (A). The molar extinction coefficient was calculated as 1.56 x 10^4 mol^{-1} dm^3 cm^{-1}. The latter value is within 85% of the value provided by the supplier[1].

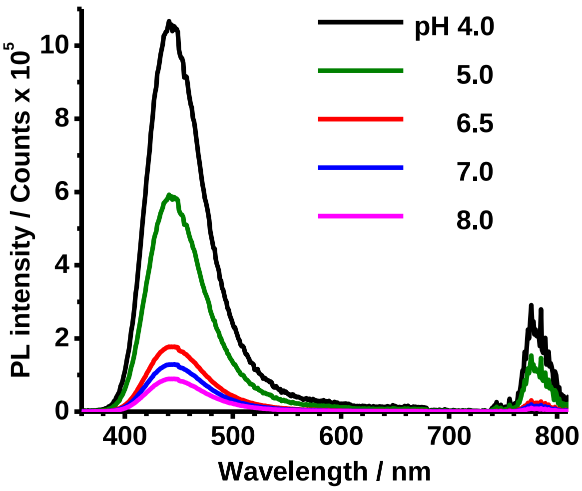

Figure S4. PL spectra for labelled DXMG-GMA gel measured at various pH values**.**

Estimation of average separation of CSS and CF particles in the injectable gels

The concentrations of the CF (C_{CF}) and CSS (C_{CSS}) particles in the gels were ~ 0.10 wt% and 3.0 x 10^{-4} wt.%, respectively. The average diameters of the particles from TEM (Fig. 1A and C) were similar (~ 85 nm). Consequently, there were approximately 300 CF particles for every CSS particle in the gels. We assume a square lattice in order to calculate the separation between CF and CSS particles for simplicity. The average separation between the CSS particles and their nearest neighbour CF particles ($H_{CF\text{-}CSS}$) is further assumed to be the same as that between neighbouring CF particles ($H_{CF\text{-}CF}$).

The following steps are used to estimate $H_{CF\text{-}CF}$ and, hence, $H_{CF\text{-}CSS}$. (1) The mass of a CF particle (m_{CF}) is calculated. (2) The number of CF particles in 1 cm^3 of gel is calculated. (3) The number of CF particles per cm (N_{CF}) is estimated using a cubic lattice. (4) The average value for $H_{CF\text{-}CF}$ is then calculated.

Step (1): Using

$$m_{CF} = \frac{\rho \pi d^3}{6} \qquad \text{(S1)}$$

where ρ and d are the density (1.0 g.cm^{-3}) and diameter (8.5 x 10^{-6} cm), it follows that m_{CF} = 3.2 x 10^{-16} g.

Step (2): The value of C_{CF} = 0.10 wt.% is equivalent to 10^{-3} g.cm^{-3}. Therefore, the value of the number of particles per cm^3 = 10^{-3} g / 3.2 x 10^{-16} g = 3.1 x 10^{12}.

Step (3): The value of N_{CF} for the cubic lattice is then $(3.1 \times 10^{12})^{1/3} = 1.4 \times 10^4$ cm^{-1}.

Step (4): The value for $H_{CF\text{-}CF} = 1/N_{CF} = 6.9 \times 10^{-5}$ cm = 690 nm (= $H_{CF\text{-}CSS}$)

Given the value for d above of 85 nm, the average CF to CSS surface separation is ~ 600 nm.

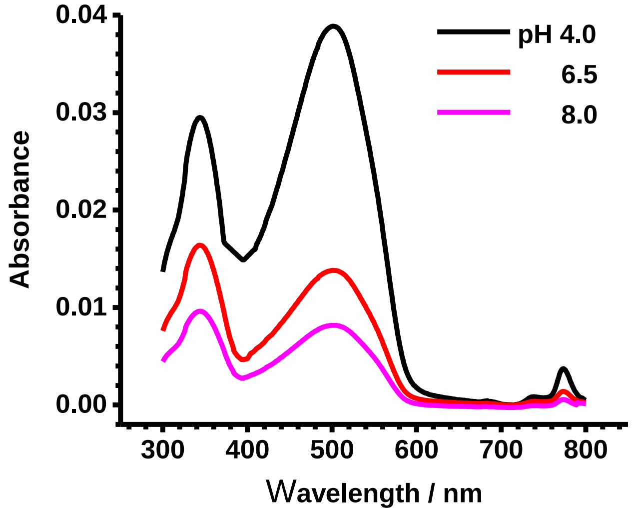

Figure S5. UV-visible spectra for labelled DXMG-GMA gel obtained at various pH values.

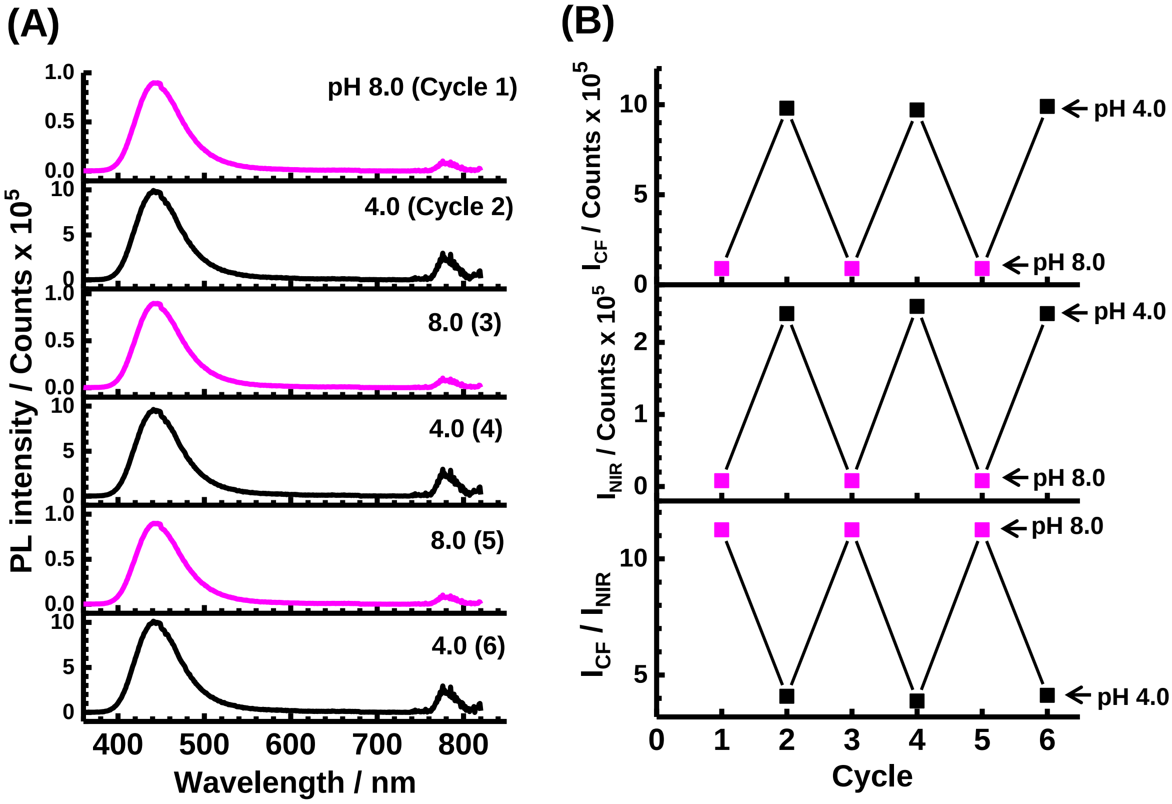

Figure S6. (A) PL spectra and **(B)** PL intensity of the CF and NIR peaks at pH 4.0 and 8.0 for labelled DXMG-GMA gel measured during pH switching.

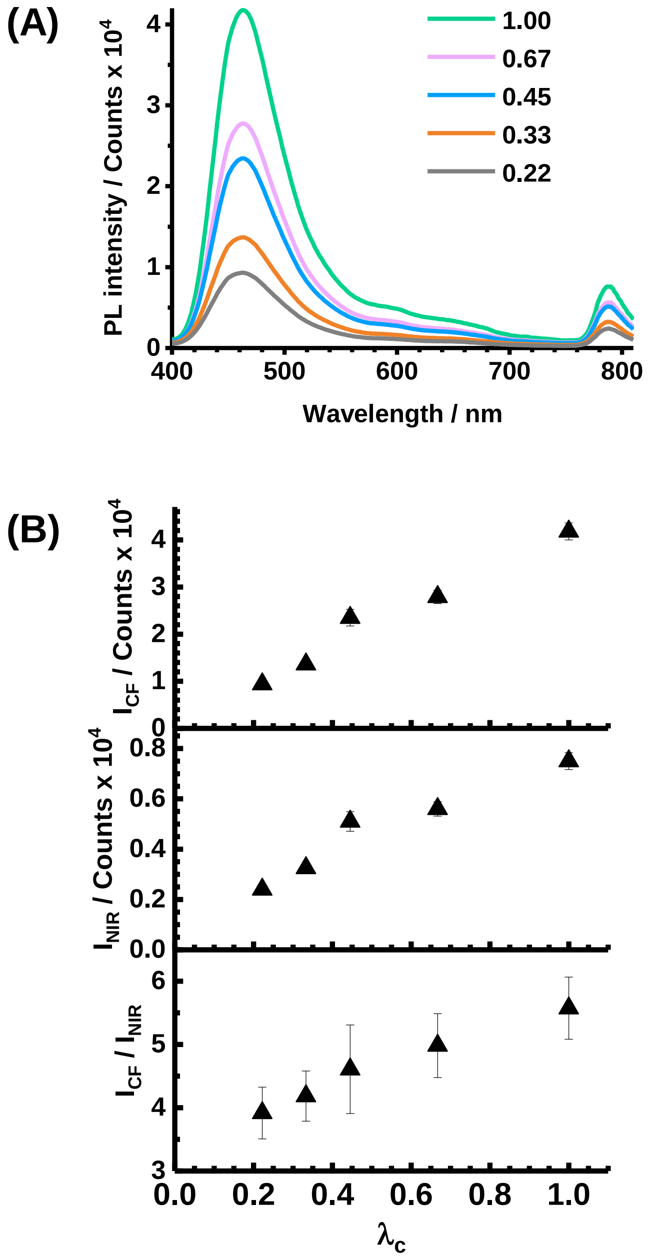

Figure S7. **(A)** As-measured PL spectra for labelled PEI-MG during compression. The compression deformation ratios (λ_c) are shown in the legend. **(B)** Variation of I_{CF}, I_{NIR} and I_{CF}/I_{NIR} with λ_c. The error bars for some of the points in (B) are smaller than the symbols.

Equation relating deformation ratio during compression to fluorescence intensity

To obtain an equation that relates the PL emission intensity to the compressive deformation ratio (λ_c) the geometry depicted in Fig. S8 is used. (Note that $\lambda_c \leq 1.0$.) The parameters I_{ex}, $I_{em(0)}$ and $I_{em(c)}$ are the intensities of the excitation beam, emission from the gel in the initial (non-compressed) state and emission in the compressed state, respectively. The parameters t_o, t_c, L_o and L_c are the non-compressed thickness, compressed thickness, non-compressed path length and compressed path length, respectively. The angle (θ) is the angle between the incident excitation beam and the emitted beam. Furthermore, $\theta/2$ corresponds to the normal.

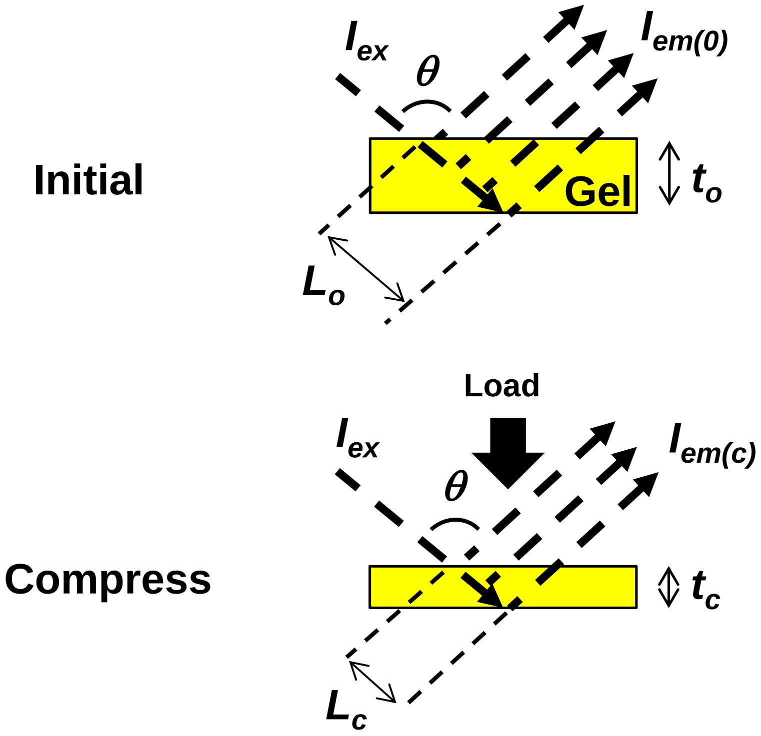

Figure S8. Geometry for a PL experiment involving a gel before and during compression.

Considering the geometry in Fig. S8 it follows that provided θ is constant:

$$\frac{L_c}{L_o} = \frac{t_c}{t_o} = \lambda_c \qquad \text{(S2)}$$

Because the path length decreases during compression the total number of CSS and CF particles illuminated also decreases. Assuming that I_{em} ~ number of CSS or CF particles probed by the incident beam (which will be proportional to the path length) it follows that:

$$\lambda_c = \frac{I_{em(c)}}{I_{em(0)}} \qquad \text{(S3)}$$

Equation (S3) shows that the ratio of the emitted PL intensities for the CF or NIR particles within the gel should equal the compression deformation ratio. If this relationship holds then it should be possible to remotely estimate the deformation of the compressed gels using PL.

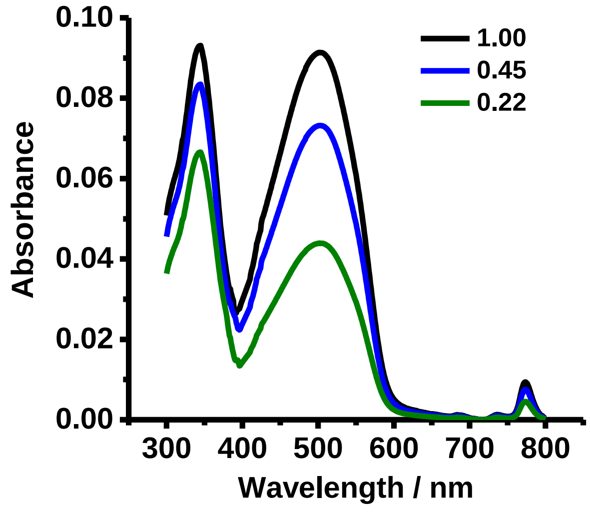

Figure S9. UV-visible spectra for labelled PEI-MG gel obtained at various λ_c values.

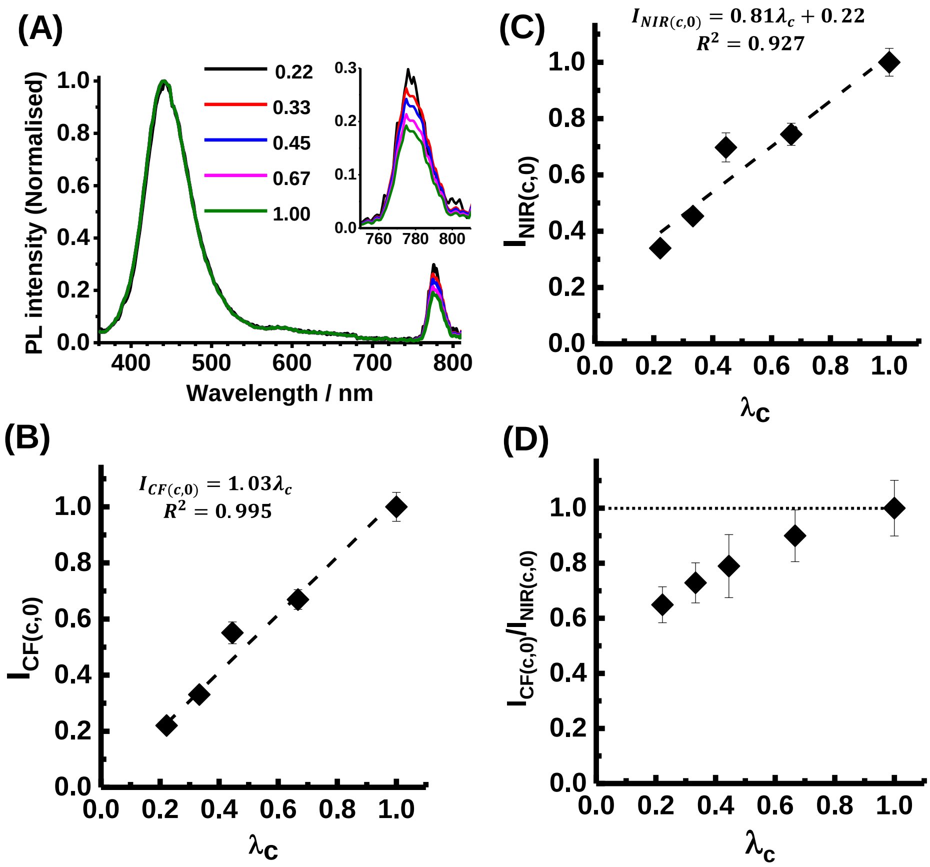

Figure S10. (A) Normalised PL spectra for labelled DXMG-GMA gel at different λ_c values. **(B)** and **(C)** show normalised PL intensities for the PL peaks from (A) plotted against λ_c. **(D)** Normalised ratios for the CF and NIR intensities versus λ_c.

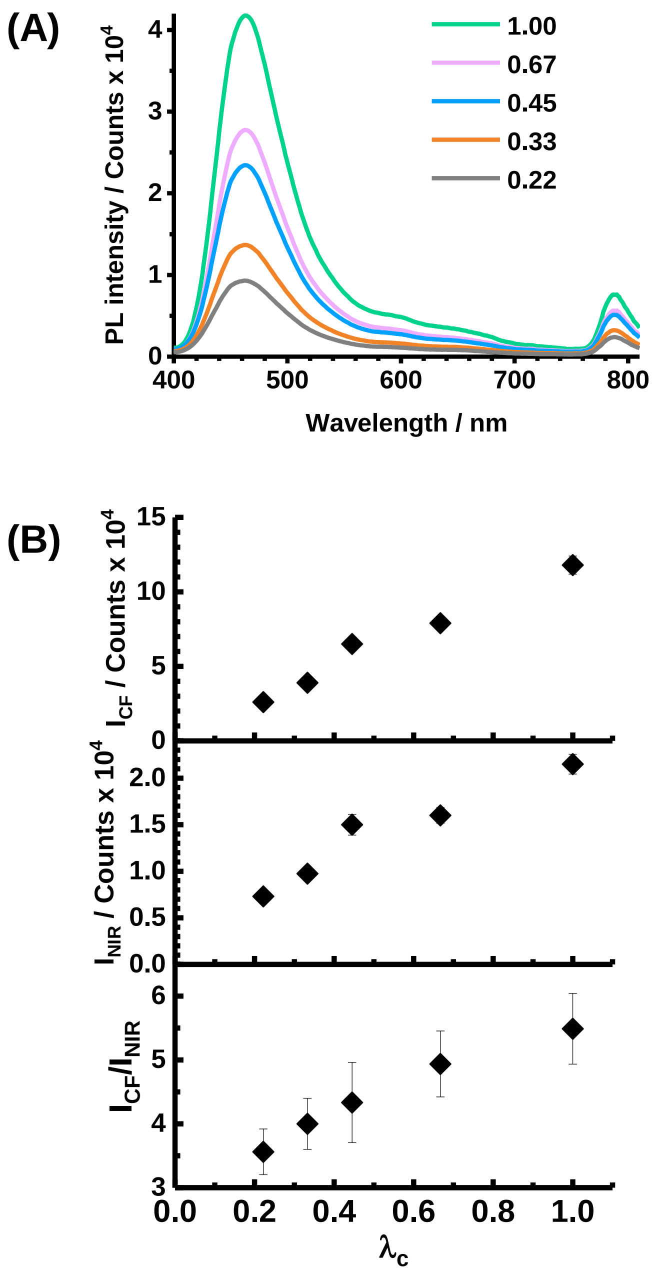

Figure S11. **(A)** As-measured PL spectra for labelled DXMG-GMA during compression. **(B)** Variation of I_{CF}, I_{NIR} and I_{CF}/I_{NIR} with λ_c. The error bars for some of the points in (B) are smaller than the symbols.

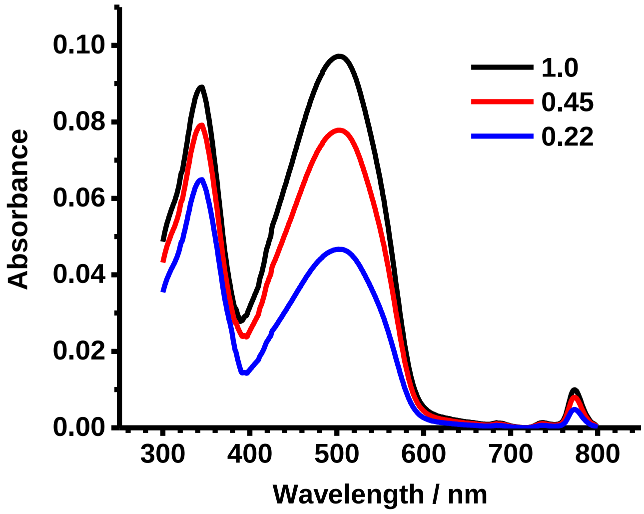

Figure S12. UV-visible spectra for labelled DXMG-GMA gel obtained at various compressive compression deformation ratios.

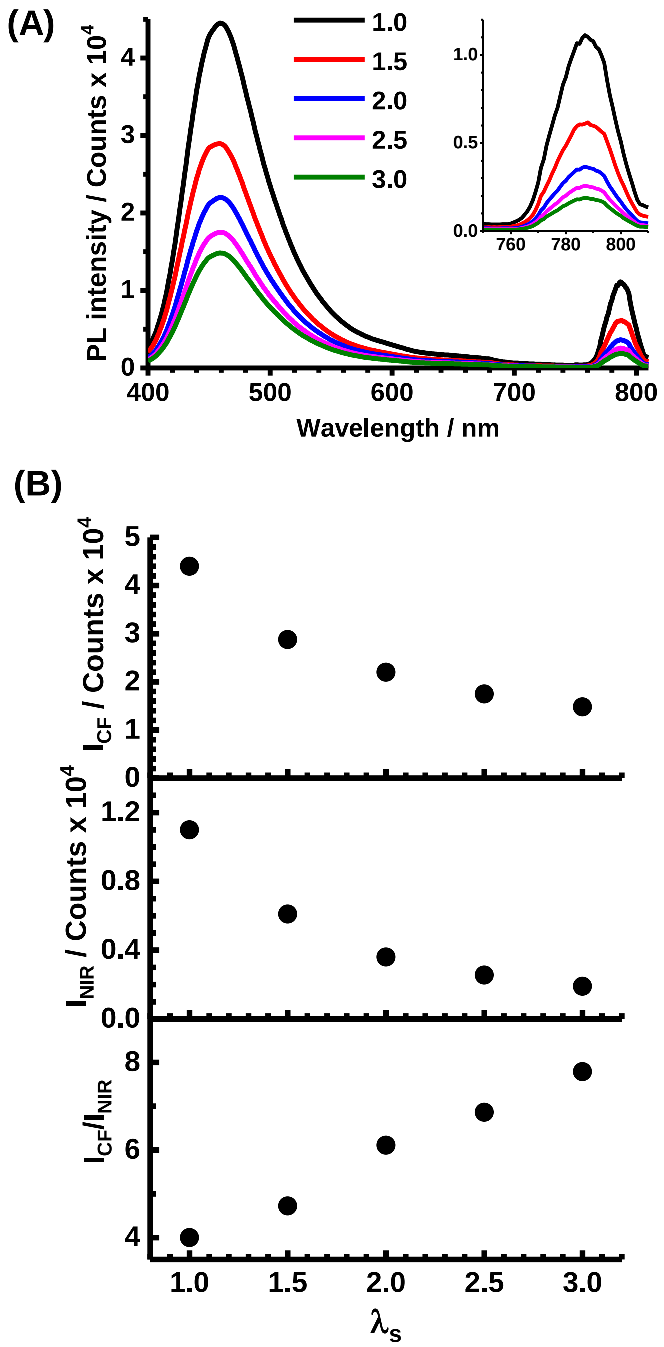

Figure S13. **(A)** As-measured PL spectra for labelled PEI-MG during tension. **(B)** Variation of I_{CF}, I_{NIR} and I_{CF}/I_{NIR} with tensile deformation ratio (λ_s).

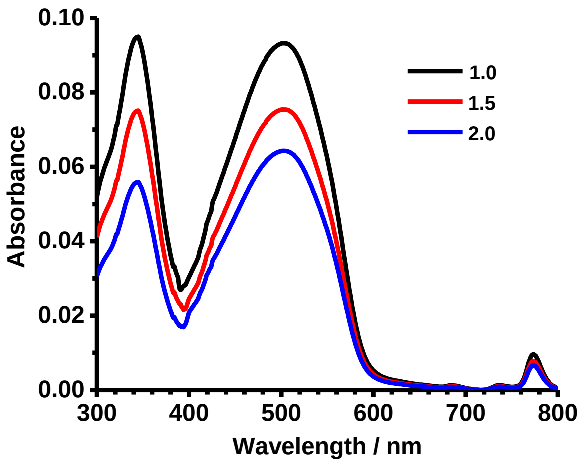

Figure S14. UV-visible spectra for labelled PEI-MG obtained at various λ_s values.

Reference

1. *www.biotium.com/technology/cf-dyes/cf350-dye/ Accessed Sept 09, 2020*.